GENIORS

Research and Innovation Action (RIA)

This project has received funding from the European Union's Horizon 2020 research and innovation programme under grant agreement No 755171.

Start date : 2017-06-01 Duration : 48 Months
http://geniors.eu/

contribution of computational multi- disciplinary approaches to the design of solvent extraction devices

Authors : Pr. Hanson BRUCE (Leeds University), Dr Andrea de Santis (ULEEDS), Prof. Bruce C Hanson (ULEEDS)

GENIORS - Contract Number: 755171

Project officer: Roger Garbil

Document title	contribution of computational multi- disciplinary approaches to the design of solvent extraction devices
Author(s)	Pr. Hanson BRUCE, Dr Andrea de Santis (ULEEDS), Prof. Bruce C Hanson (ULEEDS)
Number of pages	25
Document type	Deliverable
Work Package	WP5
Document number	D5.4
Issued by	Leeds University
Date of completion	2020-10-14 14:20:30
Dissemination level	Public

Summary

Modified report.

Approval

Date	By
2020-10-14 19:52:03	Pr. Christian EKBERG (Chalmers)
2020-10-15 09:16:17	Dr. Jean-Marc ADNET (CEA)
2020-11-13 11:30:13	Mr. Stéphane BOURG (CEA)

GENIORS

GEN IV integrated oxide fuels recycling strategies

D5.4 Contribution of computational multi-disciplinary approaches to the design of solvent extraction devices

Author(s): A De Santis (ULEEDS)

Version: 0 issued on 07/09/2020

Work Package 5

University of Leeds

Andrea De Santis

Contributors

Work contribution to the following Domains and Work-Packages

☐	DOMAIN 1 WP1	☐	WP2	☐	WP3	☐	WP4
X	DOMAIN 2 WP5	☐	WP6	☐	WP7		

☐	DOMAIN 3 WP8	☐	WP9	☐	WP10
☐	DOMAIN 4 WP11	☐	WP12	☐	WP13

CONTENTS

This project has received funding from the EURATOM research and training programme 2014-2018 under grant agreement No 730227

INTRODUCTION

Liquid-liquid extraction is a key process in standard spent nuclear fuel reprocessing methods such as PUREX as well as in advanced reprocessing technologies foreseen in for the next generation of nuclear power plants [1]. Intensified liquid-liquid extraction, which is attained in devices such as pulsed sieve-plate extraction columns and Annular Centrifugal Contactors (ACCs), allows for higher extraction efficiencies and lower residence times compared to the standard extraction process taking place in devices such as mixer-settlers [2] [3].

In particular, ACCs are regarded as a promising technology due to their high mass transfer rates and good separation efficiency. However, they are characterised by a highly complex hydrodynamic behaviour and there is a general lack of understanding of the local features of the multiphase flow as well as of the local droplet size distribution found in these devices [4].

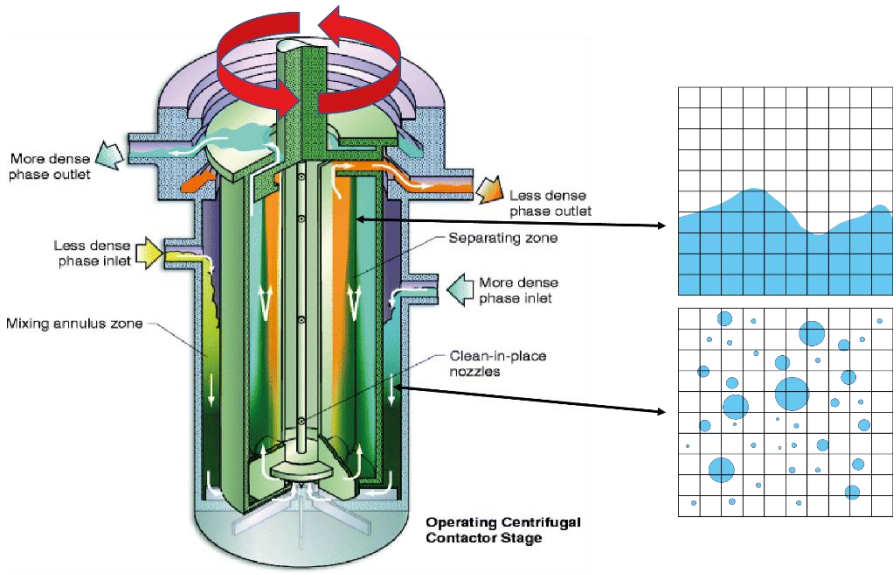

Figure 1. Schematic of an ACC (left) and qualitative representation of interface-resolving (top-right) and interface-averaging (bottom-right) approaches.

A schematic representation of an ACC is provided on the left-hand side of Figure 1. Both the aqueous and the organic phases enter the device in the mixing region, i.e. in the annular section encompassed by the outer case and the external rotor wall. Due to the high-speed rotation imparted by the rotor the mixing region is dominated by a Taylor-Couette-type multiphase flow and the mixture inside the annulus is subject to high shear and turbulence. This results in the formation of a fine dispersion, which is highly desirable to enhance the mass transfer of the solute to the solvent. This finely dispersed mixture is collected at the bottom of the device and then guided within the rotor by means of dedicated vanes. Coalescence and phase separation take place by means of the different centrifugal force experienced by the two phases within the rotor due to their different density. At the top of the rotor, the two phases are collected and guided to their outlet sections by means of a complex weir system.

Computational Fluid Dynamics (CFD) has the potential to allow for in-silico investigation of ACCs and thus shed light on the intricate hydrodynamics of these devices. However, this is hindered by the complexity of the flow to be simulated, which precludes the use of standard “off-the-shelf” modelling approaches for multiphase flows [5].

This project has received funding from the EURATOM research and training programme 2014-2018 under grant agreement No 730227

Broadly speaking, multiphase modelling approaches can be divided in two main categories [6] [7]:

- Interface-averaging approach
- Interface-resolving approach

The interface-averaging approach results in the so-called multifluid (or Eulerian) models; in these models it is assumed that scale separation exists between the continuous and the dispersed phases; this allows for conditional volume averaging of the governing equations and therefore in this approach the interface morphology is not directly resolved. All the phases within the system, which share the same pressure, are represented as interpenetrating continua and each phase has its own momentum equation. Due to the averaging procedure and consequent loss of information on the interface morphology, suitable closures are needed for the exchange of momentum, heat and mass at the interface.

The interface-resolving approach seeks to directly resolve the morphology of the interface between the phases; therefore, the numerical grid has to be fine enough to allow for an adequate resolution of the interface, which hinders the application of this approach to finely dispersed flows. Two main model classes stem from this approach: interface-tracking models which track the evolution of the interface in a Lagrangian fashion, and interface-capturing models which reconstruct the interface from a known indicator function. Interface-capturing models include both the Level Set [8] and the Volume of Fluid (VoF) [9] techniques; the latter technique, in particular, is fairly numerically robust and widely used in the simulation of segregated multiphase flows, but tends to show some degree of interface smearing due to the numerical diffusion of the indicator function. Therefore, a special numerical treatment is required to counteract this “unphysical” smearing and to retain the sharpness of the interface.

From the description of the operating principles of ACCs, and as schematically shown on in Figure 1, it follows that the interface-averaging approach is better suited for the simulation of the finely dispersed flow observed in the mixing region, whilst an interface-resolving approach is desirable for the simulation of the segregated flow found within the rotor. This highlights the problems encountered when trying to apply modelling paradigms suitable for “idealized” flow configurations, such as the fully dispersed and the large-scale/segregated interface assumptions, to “real-life” complex flows. This has been demonstrated in the context of liquid-liquid extraction in the recent LES/VoF simulation of a Pulsed Sieve-plate Extraction Column reported in [10]. It has been observed that an extremely fine mesh, associated with an unfeasible computational cost, would be required to resolve the single droplets within the system following an interface-resolving approach; including the effects of the presence of these droplets, on the other hand, is key for the correct representation of the hydrodynamic behaviour and of the mass transfer within the system. [11] came to the same conclusion following a LES/VoF investigation of the CINC-V2 ACC. Therefore, it is clear that there is a need for a generalized multiphase modelling approach capable of switching between some form of the two different modelling paradigms, interface-resolving and interface averaging, based on the local flow conditions and mesh resolution [6] [12] [13].

In this context, the University of Leeds has developed a novel Generalized Multifluid Modelling approach (GEMMA) [14]. This approach relies on the multifluid modelling framework for the solution of the governing equations (i.e. each phase retains its own momentum equation, and therefore suitable models are needed to account for the exchange of momentum between the different phases) and uses a local binary switch to identify the local interfacial morphology as a function of the ratio between the local interfacial scales and the local mesh resolution. Including a dependency on the local mesh resolution is crucial since, in the modelling context, “small” and “large” interfacial scales are always defined with respect to the local mesh size. The status of the switch then allows for the activation/deactivation of different terms and models in the governing equations; in the regions of small/dispersed interfacial scales a standard multifluid formulation is recovered,

This project has received funding from the EURATOM research and training programme 2014-2018 under grant agreement No 730227

whilst a multifluid adaption of the interface-resolving approach is employed. A more in-depth description of the modelling concept is given in the next section.

THE GEMMA CONCEPT

The GEMMA method has been implemented in the open-source CFD code OpenFOAM v7.0 [15] [16]. The OpenFOAM's built-in *reactingMultiphaseEulerFoam* solver has been used as a starting point for the implementation of GEMMA. This is a multifluid solver for n compressible phases and can account for both heat and mass transfer. The solver also includes a broad variety of models for the interfacial transfer of momentum, heat and mass and can be coupled to an inhomogeneous population balance [17] to evaluate the local size distribution of the dispersed phase. Assuming incompressible phases, and neglecting heat and mass transfer, the momentum conservation equation for phase k is given by the standard multifluid formulation

$$\frac{\partial \alpha_k \boldsymbol{u_k}}{\partial t} + \nabla \cdot (\alpha_k \boldsymbol{u_k} \boldsymbol{u_k}) = -\alpha_k \nabla p/\rho_k + \nabla \cdot (\nu_k \alpha_k \nabla \boldsymbol{u_k}) + \alpha_k \boldsymbol{g} + \left(\boldsymbol{F_k} + \boldsymbol{F_{st,k}}\right)/\rho_k \quad (1)$$

where both the interfacial momentum exchange $\boldsymbol{F_k}$ includes forces due to drag, lift, wall lubrication and turbulent dispersion and the surface tension force $\boldsymbol{F_{st,k}}$, included in Equation (1) for reasons that will be clear later, is taken equal to zero in the standard multifluid formulation.

Under the same assumptions, the continuity equation for phase k reads

$$\frac{\partial \alpha_k}{\partial t} + \nabla \cdot (\alpha_k \boldsymbol{u_k}) = 0 \quad (2)$$

The GEMMA approach relies on the introduction of a binary switch C_α on top of the standard multifluid formulation of *reactingMultiphaseEulerFoam*. The switch is equal to zero in the cells where the interfacial scales are smaller than the local mesh resolution; this makes a direct resolution of the interface morphology not feasible in those cells. In these cells, the GEMMA formulation is effectively equivalent to a standard multifluid approach, summarised by Equations (1) and (2). The closures used to evaluate the different contributions (drag, lift, wall lubrication and turbulent dispersion) to the interfacial momentum transfer term $\boldsymbol{F_k}$ are the standard models derived under the assumption of the presence of a dispersed phase (i.e. of several Dispersed Phase Elements (DPEs) such as droplets or bubbles, often assumed to have spherical shapes) embedded in a continuous phase. An example of such a closures is the well-known Schiller-Naumann correlation to evaluate the drag coefficient for spherical DPEs [18]. In these cells, the surface tension force $\boldsymbol{F_{st,k}}$ is taken equal to zero.

In the regions of large/segregated interfacial scales the binary switch C_α is equal to one. The standard interfacial momentum exchange closures, which have been developed under the assumption of the presence of a dispersed phase made up of Dispersed Phase Elements (DPEs) such as droplets or bubbles, are no longer applicable. Furthermore, the mesh size in these regions theoretically allows for a direct resolution of the interface morphology, ideally calling for a "multifluid" version of the interface-resolving modelling approach. In GEMMA, this is achieved by:

1. Introducing an ad-hoc formulation for interfacial momentum exchange due to drag (all the other interfacial momentum exchange terms are neglected). A novel generalized blending technique, depending on the local C_α value, has been proposed to blend between interfacial exchange models suitable for small and large interfacial scales [14]

This project has received funding from the EURATOM research and training programme 2014-2018 under grant agreement No 730227

2. Introducing a form of interface compression to reduce interface "smearing" due to numerical diffusion
3. Introducing a multifluid version of the Continuum Surface Force (CSF) to evaluate the surface tension force $\boldsymbol{F_{st,k}}$

For the large-scale/segregated drag force, the closure proposed by [6] is employed, which expressed the drag force between phases i and j in the regions of large-scale interfacial scales (LI) as

$$\boldsymbol{F_{d,LI}} = \left[0.5\frac{\rho_m \delta|\boldsymbol{U_i}-\boldsymbol{U_j}|}{\frac{\alpha_i\alpha_j\mu_i\mu_j}{\mu_i+mu_j}} + 8\frac{\frac{\alpha_i\alpha_j\mu_i\mu_j}{(\alpha_j\mu_j+\alpha_j\mu_i)}}{\frac{\mu_i\mu_j}{(\mu_i+\mu_j)}}\right]\frac{|\nabla\alpha|}{\delta}\frac{\mu_i\mu_j}{(\mu_i+\mu_j)}(\boldsymbol{U_i}-\boldsymbol{U_j}) \quad (3)$$

The numerical diffusion of the interface is counteracted by including a compressive terms in Equation (2), which is a popular method employed in VoF [19]. The modified continuity equation including the compressive term reads

$$\frac{\partial\alpha_k}{\partial t} + \nabla\cdot(\alpha_k\boldsymbol{u_k}) + \nabla\cdot\left(\boldsymbol{u_c}\alpha_k(1-\alpha_k)\right) = 0 \quad (4)$$

where the term $\alpha_k(1-\alpha_k)$ ensures that the compressive term is only active in the interface region and is $\boldsymbol{u_c}$ the compressive velocity. It is has to be pointed out that the compressive term appearing in Equation (4) does not corresponds to any actual physical phenomenon, but is merely a numerical expedient using to counteract another purely numerical effect, i.e. the "smearing" of the interface. The compressive velocity $\boldsymbol{u_c}$ is expressed as

$$\boldsymbol{u_c} = C_\alpha|\boldsymbol{u}|\frac{\nabla\alpha}{|\nabla\alpha|} \quad (5)$$

where $\frac{\nabla\alpha}{|\nabla\alpha|}$ ensured that $\boldsymbol{u_c}$ is normal to the interface, and $|\boldsymbol{u}|$ is the magnitude of the relative velocity between the two phases at the interface. C_α is a numerical coefficient which is usually taken equal to 1 in VoF; in the GEMMA approach C_α corresponds to the binary switch, which ensures that interface compression is only active in the large-interface cells.

The surface tension force $\boldsymbol{F_{st,k}}$ is evaluated using an ad-hoc multifluid extension of the well-known CSF method [20], which is usually employed in the interface-resolving framework to account for surface tension effects in the momentum equation. Including the density correction term proposed by [21], the surface tension force is expressed as

$$\boldsymbol{F_{st}} = \sigma\kappa\nabla\alpha\frac{2\rho}{\Delta\rho} \quad (6)$$

where ρ is the local mixture density, $\Delta\rho$ is the density difference between the two phases, σ is the surface tension coeffcient and κ is the local interface curvature, evaluated as

$$\kappa = -\nabla\cdot\left(\frac{\nabla\alpha}{|\nabla\alpha|}\right) \quad (7)$$

In order to avoid numerical problems in the evaluation of the gradient of the sharp volume fraction field, it is common practice to employ a smoothed volume fraction field in the evaluation of the interface curvature.

This project has received funding from the EURATOM research and training programme 2014-2018 under grant agreement No 730227

Within GEMMA, this is achieved using the Smoothed Continuum Surface Force (SCSF) method of [22], where the volume fraction field is smoothed by successive interpolation cycles from cell centres to cell faces.

Finally, one should note that CSF-based methods have been derived to be used in the one-fluid framework, where all the phases share the same momentum equation. In the multifluid approach, the total surface tension force given by Equation (6) should be somehow distributed among the phases occupying a given mesh cell. [23] showed that an effective way to achieve this is to use the local phase volume fraction α_k as a weighting factor. Furthermore, in the context of "hybrid" models, one should be careful to only include surface tension effects when working in large-interface mode; within GEMMA, this is achieved by multiplying the surface tension force resulting from the modelling assumptions outlined above by the switching function C_α, resulting in the following formulation for the surface tension force for phase k

$$\boldsymbol{F_{st,k}} = \alpha_k \sum_{i=1}^{n_k} \left(C_{\alpha_{k,i}} \sigma_{k,i} \kappa \nabla \alpha \frac{2\rho}{\Delta \rho_{k,i}} \right) \tag{8}$$

LARGE-INTERFACE/DISPERSED-INTERFACE SWITCH

The main idea behind the switching logic used in GEMMA is to link the activation of the large-interface mode to the local resolution of the interface morphology. Specifically, the large-interface mode should only be activated in regions where a desired resolution of the interface is achieved. This is quantified by introducing the Interface Resolution Quality (IRQ) index, originally proposed by [24], within the switching logic. IRQ is defined as

$$IRQ = \frac{2}{\Delta \kappa} \tag{9}$$

where $\Delta = \sqrt[3]{V}$ is the local mesh size.

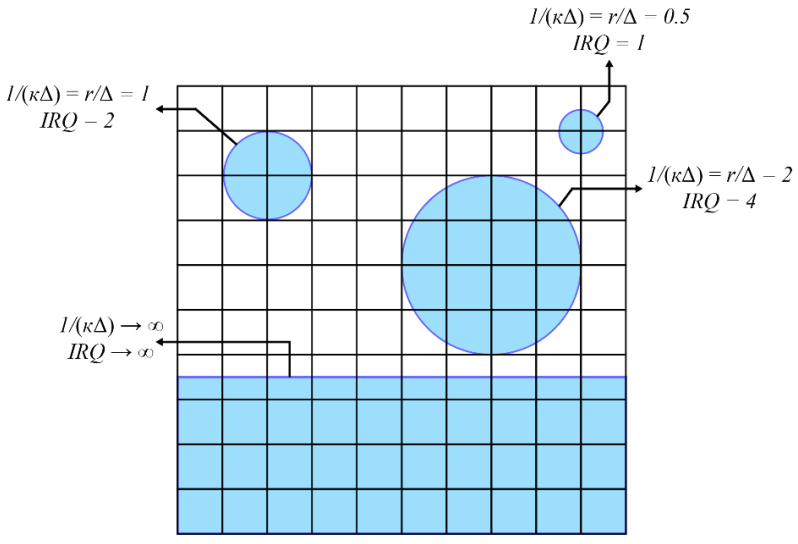

Figure 2. Two-dimensional representation of the IRQ criterion for circular DPEs of different size and for a segregated interface morphology.

A schematic representation of the meaning of IRQ is provided in Figure 2. The figure makes use of the observation that, for a spherical DPE, it results $\kappa = 1/r$; it can be seen that large values of IRQ correspond to a more accurate resolution of the interface. Therefore, the switching criterion in GEMMA relies on the introduction of a minimum threshold IRQ_{crit}; the local IRQ value has to be higher than the critical value

This project has received funding from the EURATOM research and training programme 2014-2018 under grant agreement No 730227

specified by the user. In addition, minimum and maximum thresholds for the value of the dispersed phase volume fraction are introduced within the switch logic; threshold values of 0.01 for α_{min} and 0.99 for α_{max} are used in all the simulations performed in this work to ensure that interface-resolution is only activated in the proximity of the interface.

When the diameter of the dispersed phase d in interface-averaging mode is known, for example from the solution of a population balance equation, an additional check is performed to ensure that interface resolution is only switched on in the cells where the condition

$$d > \Gamma\Delta \tag{10}$$

is satisfied, i.e. where the dispersed phase diameter is larger than the local mesh size by at least a factor Γ; the latter is a user-specified parameter which allows further control by guaranteeing that each DPEs is resolved by at least Γ mesh elements for the multifluid interface-resolving mode to be activated.

REDUCED POPOULATION BALANCE

As mentioned in the introduction, a knowledge of the droplet size distribution in the mixing region is key for the hydrodynamic characterisation of ACCs and also for the evaluation of their performance in terms of mass transfer. For this reason, a reduced population balance approach is embedded within GEMMA to evaluate the DPE size distribution when working in dispersed-interface mode.

The reduced population balance is based on the One Primary One Secondary Particle Method (OPOSPM) [25], which is a special instance of the Sectional Quadrature Method of Moments (SQMOM) in which only one primary particle and one secondary particle are considered [25] [26]. In the OPOSPM approach two low-order moments can be conserved, and the secondary particle represents a Lagrangian fluid particle carrying information about the droplet population through its low-order moments. Although the selection of these moments is arbitrary, the total number and volume concentrations are the most natural candidates for the conservation of the total number and mass of droplets. Because the total number and volume concentrations are conserved, the population density is represented by a single particle (assumed to have a spherical shape) whose size is given by

$$d_{30} = \sqrt[3]{\frac{m_3}{m_0}} = \sqrt[3]{\frac{6\alpha_d}{\pi N_d}} \tag{11}$$

where α_d and N_d are the volume fraction and the particle number density of the dispersed phase, respectively, which are related to the zeroth and third moment of the distribution m_0 and m_3. The dispersed phase volume fraction is already known from the solution of the related continuity equation, so the OPOSPM only requires the solution of an additional conservation equation for N_d, which reads

$$\frac{\partial(\rho_d N_d)}{\partial t} + \nabla \cdot (\rho_d \boldsymbol{u_d} N_d) = \rho_d S \tag{12}$$

where the source term is given by

This project has received funding from the EURATOM research and training programme 2014-2018 under grant agreement No 730227

$$S = (N_d - 1)g(d_{30}) - \frac{1}{2}a(d_{30}, d_{30})N_d^2 \quad (13)$$

In the equation above, $g(d_{30})$ and $a(d_{30}, d_{30})$ represent the break-up and coalescence rates, respectively, which have to be evaluated by using a suitable closure. In all the cases considered in this report, the break-up model of [27] and the coalescence model of [28] have been used.

The OPOSPM population balance allows for the evaluation of d_{30}; mathematically, this is a more coherent choice compared to d_{32}, since the former is natural quadrature node whilst the latter is not. However, keeping in mind the importance of evaluating the interfacial area density a_i to assess mass transfer within the device, it is worth observing that knowledge of d_{32} would then allow to evaluate the interfacial area density as

$$a_i = \frac{6\alpha}{d_{32}} \quad (14)$$

For the simulation of ACCs, [29] proposed to use the knowledge of d_{30} directly available from the OPOSPM population balance and estimate the ratio of d_{30}/d_{32}, which for liquid-liquid dispersions in centrifugal contactors is observed to be consistently in the range of 0.75-0.8. A value of 0.76 is used throughout the simulations presented in this report.

It should be pointed out that the OPOSPM method has been used for the sake of reducing the computational overhead associated with the resolution of the population balance equation. Nevertheless, the formulation of GEMMA is fully compatible with the MUSIG [17] multigroup inhomogeneous population balance embedded within the *reactingMultiphaseEulerFoam* solver in OpenFOAM, which allows for the evaluation of the PDF of the DPEs diameter.

TESTING IN PROTOTYPICAL MULTIPHASE FLOWS

Before its application to the simulation of cases that are relevant to liquid-liquid extraction, the GEMMA method has been tested in standard multiphase test cases which are commonly used to evaluate multiphase modelling approaches. These cases are particularly focused on the valuation of the performance of the model in the presence of a large/segregated interfaces. A prototypical multiscale test case has also been considered. The results obtained for a selection of these test cases are summarised in this section.

ETHANOL DROPLET IN EQUILIBRIUM IN AIR

The generalized multifluid surface tension implementation used within GEMMA has been assessed in a simple test case proposed by [23]; the case consists of an ethanol droplet in equilibrium in air in the absence of gravity. Both fluids are treated as laminar and the simulation has been run for a flow time of 2 s. A switch based on the local IRQ value has been used, with $IRQ_{crit} = 2$.

This project has received funding from the EURATOM research and training programme 2014-2018 under grant agreement No 730227

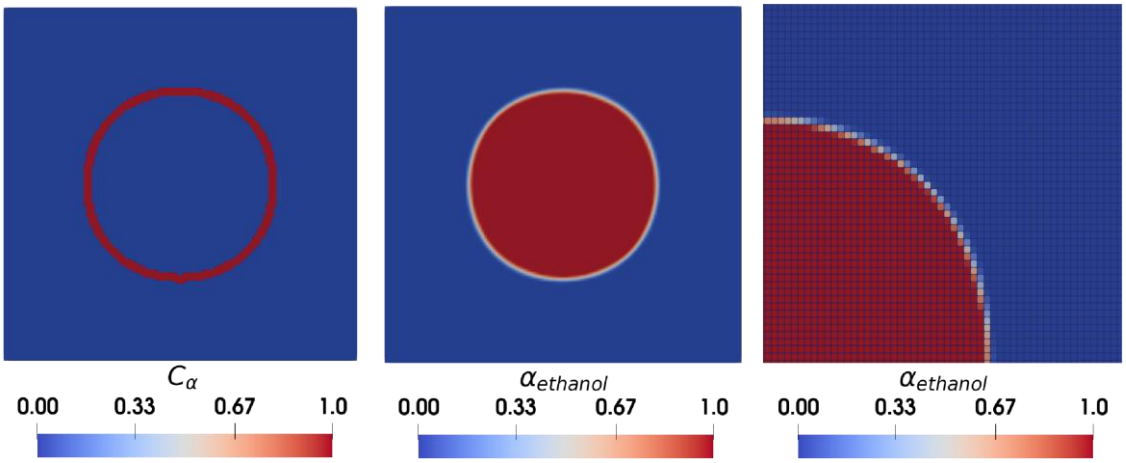

Figure 3. Contours of C_α switch (left), ethanol volume fraction (centre) and zoomed-in on the interfacial region (right).

The C_α and the ethanol volume fraction contours obtained with the GEMMA approach are shown in Figure 3. It can be seen how the switching criterion can identify the presence of the interface between the ethanol droplet and the surrounding air correctly; consequently, large-interface mode is activated in the interfacial region, as can be seen from the sharp interface visible in the zoomed-in view of the volume fraction field. This results in an interface thickness equal to approximately 2-3 times the mesh size, which is typical of interface-resolving approaches such as VoF.

The gauge pressure field $p_g = p - p_{atm}$ obtained with GEMMA is shown in Figure 4. It can be seen that the pressure field within the droplet evaluated with GEMMA is fairly smooth, which indicated that the SCSF method used to smooth the volume fraction field before the calculation of the interface curvature is effective. The analytical pressure drop across the interface for this case is equal to 11.805 Pa [23]. The average pressure within the droplet evaluated using the multifluid SCSF model (Equation (8)) is 11.45 Pa; the relative error with respect to the analytical value is -3.01%, which is in line with the accuracy of standard interface-resolving models [23] [30].

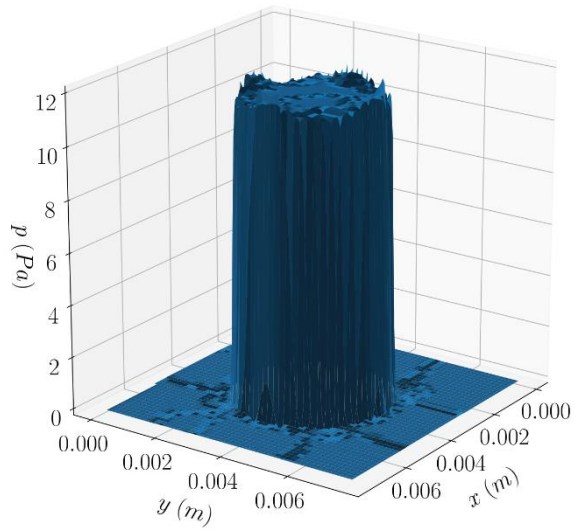

Figure 4. Gauge pressure field.

This project has received funding from the EURATOM research and training programme 2014-2018 under grant agreement No 730227

DAM BREAK IN THE PRESENCE OF AN OBSTACLE

The collapse of a water column, also known as "dam break", is a typical test case for interface-resolving models [31] [32]. The case investigated experimentally in [33], which includes the presence of an obstacle on the bottom wall, is considered here. Both the water and the air phases are considered laminar. The Schiller-Naumann drag model [18] is used for dispersed interfacial morphologies, with a constant dispersed phase diameter equal to 1 mm. The C_α switch is based on IRQ, with $IRQ_{crit} = 2$. The simulation has been run for a flow time of 1 second.

The calculated water volume fraction contours 0.2 and 0.4 seconds after the collapse of the water column are shown in Figure 5, together with the experimental snapshots from [33]; the figure also shows the local status of the C_α switch at the two flow times. The numerical results obtained with GEMMA are in good qualitative agreement with the experiment, and also in this case the switching criterion is capable of identifying the position of the segregated/large-scale interface within the domain; this results in a sharp interface being maintained in the cells where $C_\alpha = 1$, with the exception of some diffusion observed for the small water droplets present above the obstacle at t=0.2 seconds.

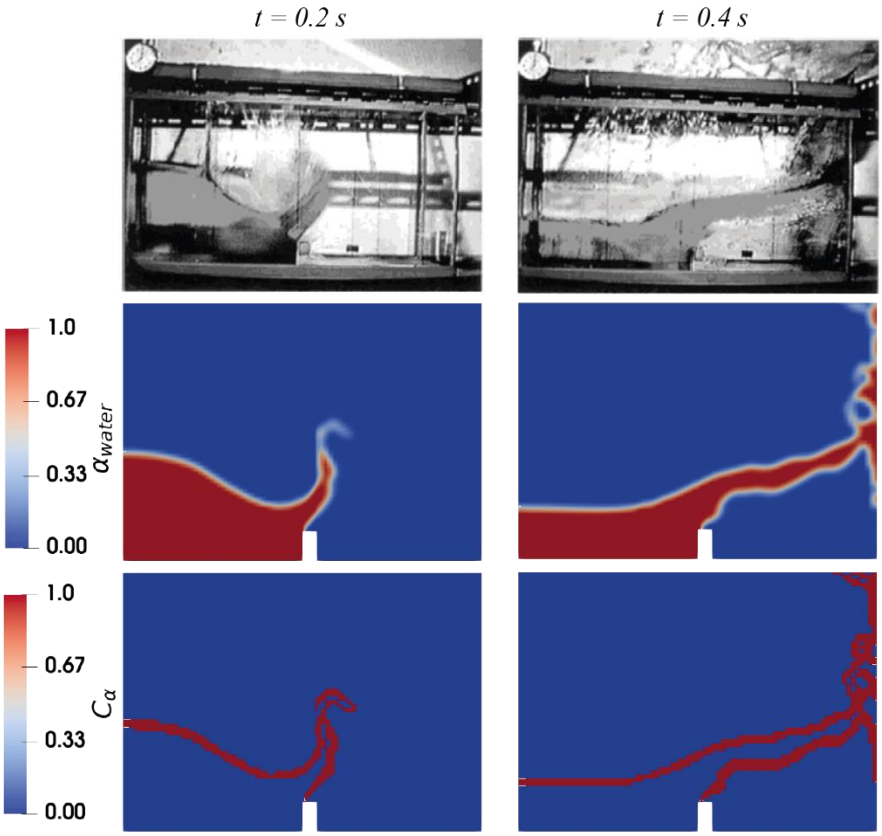

Figure 5. Experimental snapshots (top), calculated water volume fraction (centre) and C_α field (bottom) at t=0.2 and 0.4 seconds.

WATER JET PLUNGING IN A QUIESCENT POOL

A water jet plunging in a quiescent pool is a prototypical example of a multiphase flow encompassing a broad range of interfacial scales, from the segregated interface found at the free surface of the pool to the bubbles of different sizes formed by the entrained air [34]. Therefore, it is an ideal case to assess the multiscale capabilities of multiphase modelling approaches [35] [36].

This project has received funding from the EURATOM research and training programme 2014-2018 under grant agreement No 730227

For the present test with GEMMA we consider the same case and numerical set-up used in [36], which is based on the experimental set-up of [37]. The computational domain is depicted in Figure 6. Computational domain for the plunging jet case. Figure 6. The domain has a square section of side 0.1 m and a height of 0.3 m; the domain is filled with water up to 0.2 m from the bottom. The plunging water jet enters the domain through a circular pipe of diameter equal to 0.006 m with an average velocity of 1.5 m/s and a fully developed velocity profile. A constant water mass flow rate equal to that entering through the inlet pipe is enforced at the outlet, in order to keep the free surface level constant. The no-slip condition is enforced on all the walls, whilst the top surface is considered open to the atmosphere, as highlighted in Figure 6. The mesh is the same as that used by [36], and consists of about 3.03M hexahedra of 1 mm size. The air phase is considered to be laminar, whilst a LES approach with the standard Smagorinsky closure for the subgrid-scale stresses is used for the water phase [38]. A flow-time of 2 s has been simulated.

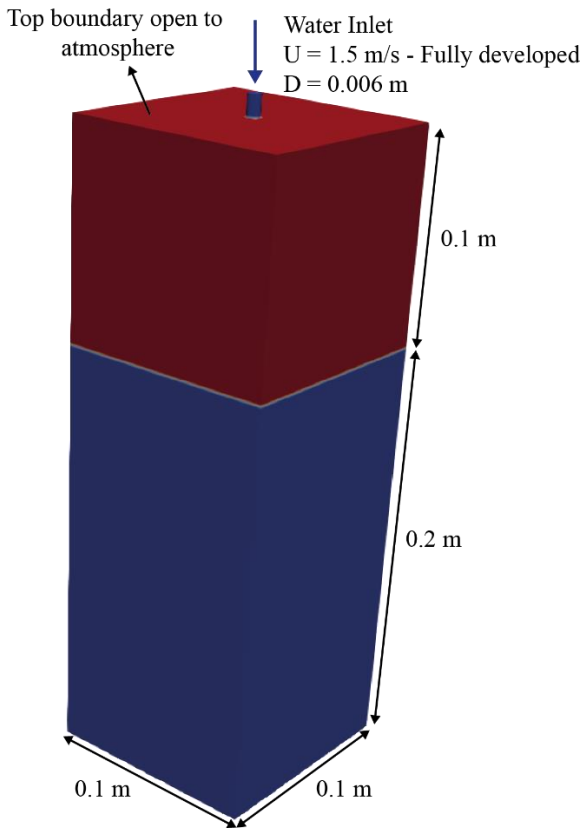

Figure 6. Computational domain for the plunging jet case.

A qualitative comparison between the numerical results and experimental snapshots reported in [31] for the initial transient up to t=0.015 seconds is reported in Figure 7. At t=0.009 seconds the jet just impinged on the free surface and there is no significant presence of entrained air bubbles; instead, a distinctive air cavity is observed in the experiments, which is well captured by the numerical simulation. It is also worth noting that the large-scale mode is activated in GEMMA for the plunging jet/air interface above the free surface as well as for the water/air interface at the free surface; in addition, interface compression is enforced for the interface between the air cavity and the surrounding water. At t=0.012 seconds pinch-off of the air cavity has happened and air bubbles start to be entrained and this is again well predicted by the simulation; interface resolution is active for the large bubble resulting from the pinch-off, whilst the smaller entrained bubbles close to the free surface are accounted for in interface-averaging mode. At subsequent instants, the large bubble deforms (t=0.014 s) and breaks down (t=0.015 s) into two smaller structures, which eventually begin to raise towards the free surface due to buoyancy; at the same time, more and more air is entrained in the form of a myriad of

This project has received funding from the EURATOM research and training programme 2014-2018 under grant agreement No 730227

relatively small bubbles. The GEMMA approach is capable to qualitatively reproducing all these phenomena; the two larger bubbles clearly visible in the experiments at t=0.015 seconds are still treated in large-interface mode, whilst the entrainment of the smaller bubbles is treated using the interface-averaging mode. After an initial transient the flow essentially consists of a downward motion caused by the plunging jet coupled with the buoyancy-driven upward motion of the bubbles surrounding the jet [37]; occasionally the entrained bubbles will coalesce and form larger cap-shaped air bubbles. All these phenomena have been qualitatively predicted in the numerical simulation performed with GEMMA.

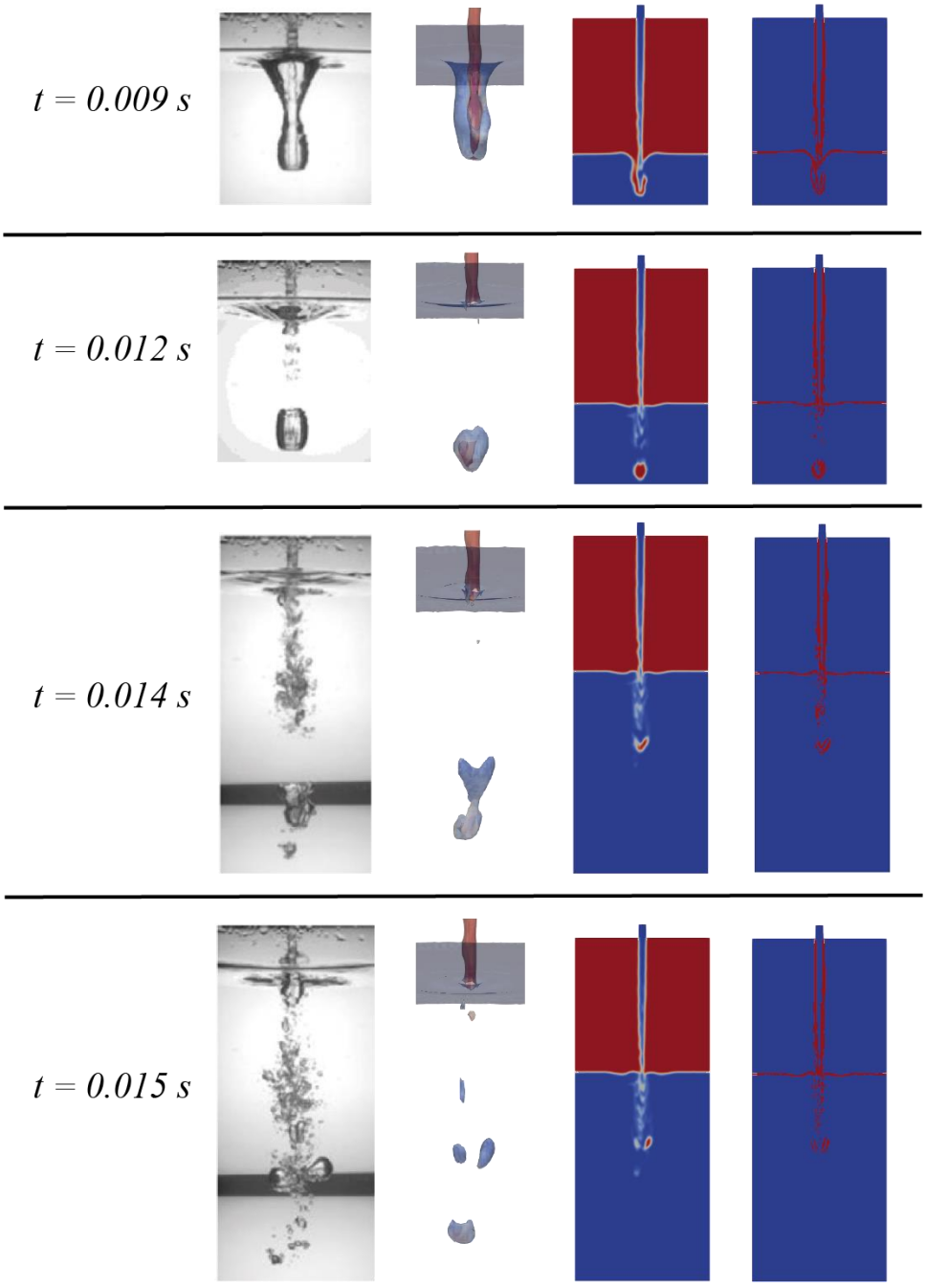

Figure 7. From left to right: experimental snapshots, isosurface of α = 0.5, air volume fraction contours on the mid-plane, C_α contours on the mid-plane at four different flow times.

This project has received funding from the EURATOM research and training programme 2014-2018 under grant agreement No 730227

SIMULATION OF THE SIMPLIFIED MIXING SECTION OF AN ANNULAR CENTRIFUGAL CONTACTOR

In order to assess the capability of the GEMMA approach with respect to the simulation of the mixing in the annular section of an ACC, this section describes the simulation of the flow in the mixing region of the CINC-V2 centrifugal contactor at different rotor speeds. This contactor has been investigated experimentally by [39]. The computational domain employed here is based on the pioneering work of [29] and consists of a 5° wedge, representing the annular region between the casing and the outer rotor wall of the contactor, with periodic conditions enforced on the wedge sides. The domain is discretized in space with a structured hexahedral mesh of size 0.4 mm, which results in a cell count of 19600. The air phase is considered to be laminar, whilst a LES approach with the standard Smagorinsky [38] closure for the subgrid-scale stresses is used for both the water and the PDMS phases. For these two phases, a wall function approach [40] is used to relax the mesh size requirements at the wall, thus resulting in a wall-modelled LES approach.

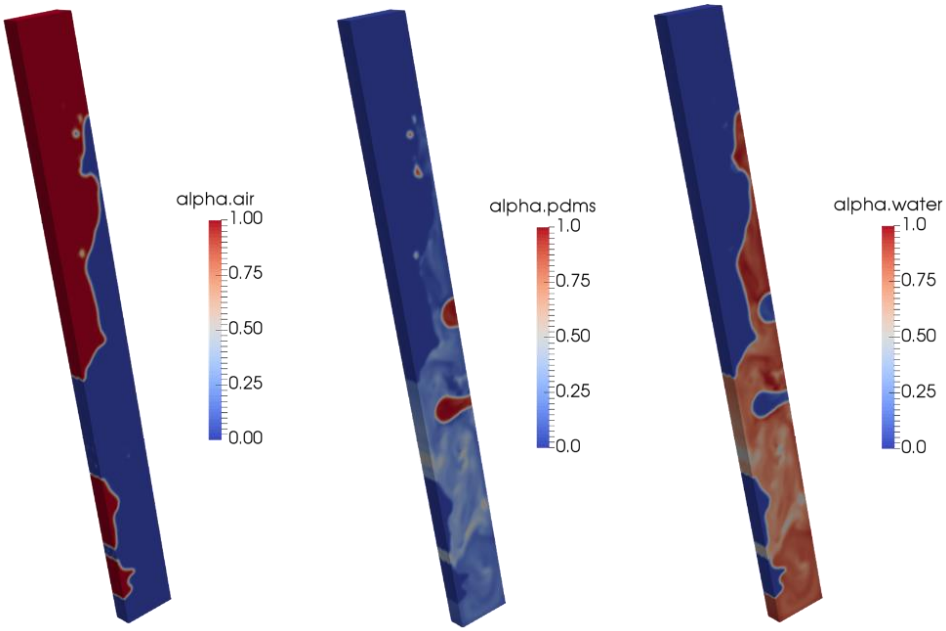

Figure 8. Instantaneous contours of air, PDMS and water volume fraction on the fine mesh.

For the baseline case, corresponding to a rotating speed of 2000 RPM, a more refined mesh of size equal to 0.2 mm (corresponding to a cell count of about 160k) has also been used to assess the sensitivity of the results to mesh resolution. All the simulations have been run for a physical time of 3 seconds, except for the cases at a rotating speed of 1100 and 1500 RPM, for which 6 seconds of physical time have been simulated. All the simulations are initialized with three horizontal layers of water, organic phase (PDMS) and air with a height ratio of 3/1/3. The GEMMA approach is used to simulate the dispersion of the organic phase in water, whilst it is assumed that a sharp interface is kept between air and the two liquid phases at all times, and hence a uniform value of 1 is C_α imposed for the air-liquid interfaces. The OPOSPM population balance approach is used to estimate the PDMS droplet size. This allowed for the use of the switching logic based on both IRQ and the dispersed phase diameter for the evaluation of the local value of C_α. The values for both IRQ_{crit} and Γ are taken equal to 2. Even though this corresponds to a coarse resolution of the interface curvature and of the dispersed droplets, respectively, this choice has been made deliberately to demonstrate to capability of GEMMA to switch between large-interface and small/dispersed-interface mode in such a flow configuration.

This project has received funding from the EURATOM research and training programme 2014-2018 under grant agreement No 730227

A snapshot of the instantaneous volume fractions of the three phases at $t = 0.7\ s$ on the fine mesh for the baseline 2000 RPM rotating speed is shown in Figure 8. It can be seen that the model keeps a sharp interface between air and the two liquid phases everywhere in the domain due to the uniform unitary value of C_α . For water and PDMS, on the other hand, the model works in interface-averaging model almost everywhere, and this is due to the fine dispersion of PDMS in water induced by the rotation of the rotor. The corresponding C_α field for the water-PDMS interface and the PDMS diameter predicted by the reduced population balance are shown in Figure 9.

It can be seen how the relatively low PDMS diameter values result on C_α being zero almost everywhere in the domain, and hence in the interface-averaging behaviour shown in Figure 8. The only exception is represented by two pockets of entrained dispersed phase, for which the mesh is fine enough to switch to C_α = 1, which guarantees the sharp interface observed in in Figure 8 for this two features.

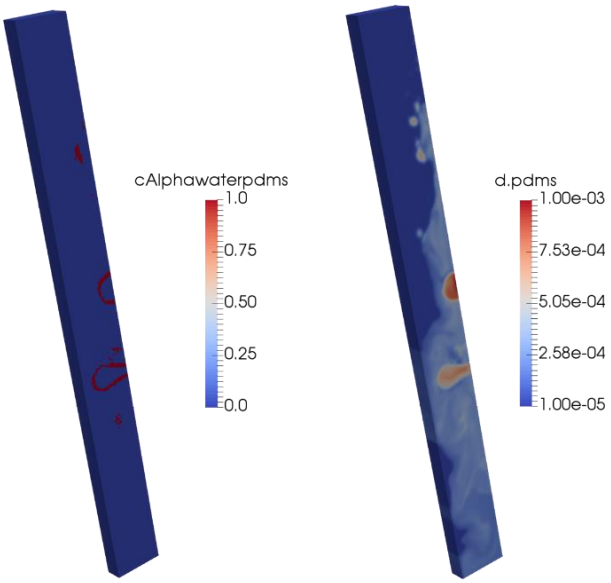

Figure 9. Instantaneous contours of water-PDMS C_α and PDMS diameter (mm) on the fine mesh.

The variation of the liquid-averaged PDMS diameter over time for the baseline 2000 RPM case is shown in Figure 10. The two meshes show similar trends for this quantity, with a time-averaged value of 248 and 252 µm for the coarse and the fine mesh, respectively, compared to an experimental value of 361 µm. When performing a quantitative comparison between the experimental and the numerical results for this quantity, one should keep in mind that the experiments have been performed on the actual contactor geometry, whilst the numerical simulations employ simplified geometry of the annular region only.

All the other rotating speeds considered in this work have been simulated on the coarse mesh only. Figure 11 shows the resulting time-averaged PDMS diameter compared with the experiments of [39]. The Sauter diameter is expected to decrease following a power-law trend with increasing rotating speeds; overall, this is the case in both the experimental and the numerical results. However, some experimental points are observed to deviate from the expected power-law curve. This is likely due to the fact that in the experimental paper d_{32} has been evaluated as the ratio between the third and the second moment of a log-normal distribution fitted to the measured droplet size distribution [39]. Thus, the experimental Sauter diameter values reported at the rotating speeds for which the fitting is less accurate are less reliable; the fit is observed to be less accurate for the two experimental points at 1500 and 2000 RPM, which explains the discrepancy with the expected power-

This project has received funding from the EURATOM research and training programme 2014-2018 under grant agreement No 730227

law trend. From Figure 11 it can be observed that the numerical results are in an overall good agreement with the experiments, especially at the higher rotation speeds. At lower rotation speeds the discrepancy between the numerical results and the experimental measurements is somehow more significant. In this respect, it should be kept in mind that the droplet size distribution gets broader at lower rotation speeds, which results in a higher standard deviation associated with the values reported at such speeds [39]. Overall, these results are seen as an encouraging demonstration of the ability of GEMMA coupled with an OPOSPM population balance to predict the complex multiphase flow observed in the mixing region of ACCs and to provide a good prediction of the expected dispersed phase diameter.

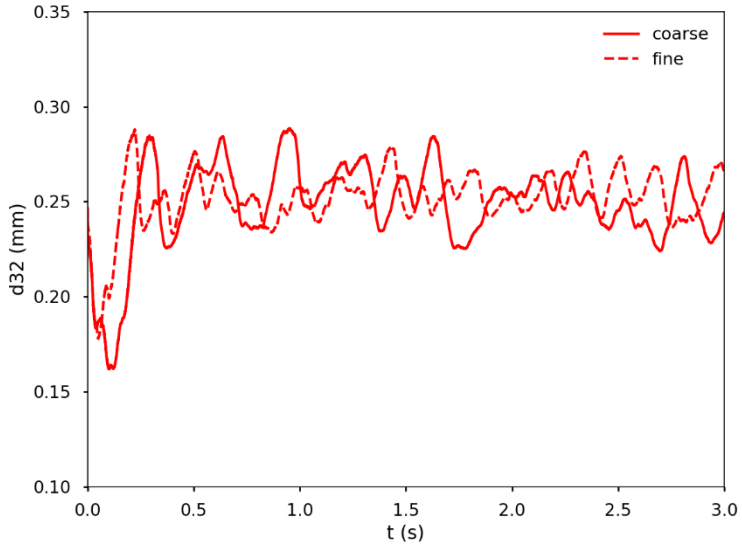

Figure 10. Transient evolution of the liquid-averaged PDMS diameter on the coarse and fine meshes at 2000 RPM.

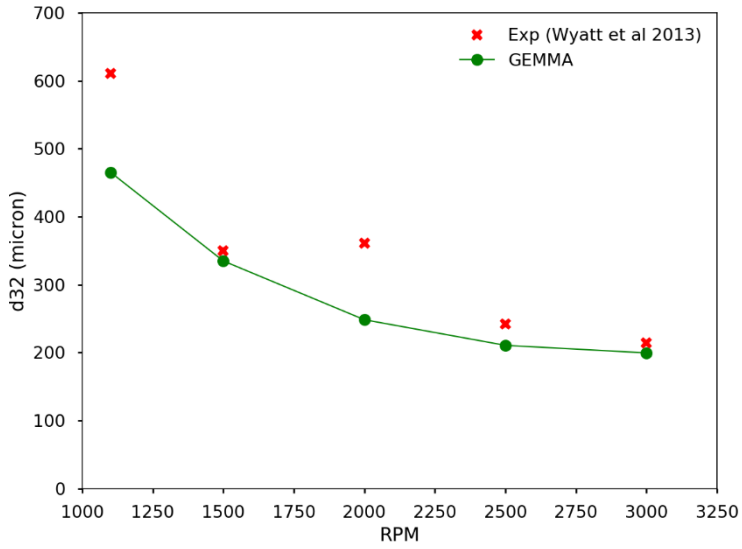

Figure 11. Measured and calculated time-averaged PDMS diameter at different rotating speeds.

This project has received funding from the EURATOM research and training programme 2014-2018 under grant agreement No 730227

SIMULATION OF A LAB-SCALE "MOCK" ANNULAR CENTRIFUGAL CONTACTOR

The previous section has shown the capability of the GEMMA modelling concept to deal with the complex flow field observed in the annular section of an ACC. This section describes the application of the modelling concept to the flow in a complete "mock" ACC. The design of this device does not replicate any specific existing ACC, and this exercise is meant to be a proof of concept to assess the capabilities of GEMMA in the simulation of a "realistic" lab-scale device. A sketch of the computational domain and of the mesh is shown in Figure 12. The outer diameter of the ACC is equal to 6.3 cm. The inner diameter of the annulus and the inner diameter of the rotor are equal to 5.4 and 5 cm, respectively. The height of the ACC is equal to 8.2 cm. The diameter of the inlet pipes is equal to 0.8 cm. Four radial vanes are present at the bottom of the device to drive the mixture within the rotor. A X-shaped stirrer is attached to the shaft within the rotor. The cut-cell mesh, shown in a mid-plane section in Figure 12, consists of 2.2M hexahedral cells.

With respect to a "real-life" ACC, the two main simplifying assumptions taken in the simulation are:

1. The complex outlet weir systems are not included in the computational domain. Instead two annular outlet sections are foreseen for the heavy phase (shown in red in Figure 12) and the light phase (shown in blue in Figure 12). An additional pressure overhead equal to 3000 Pa is imposed at the heavy phase outlet to account for the presence of the weir system that is not included in the computational model
2. The presence of the air phase is neglected in the simulation; the ACC is modelled as a two-phase system.

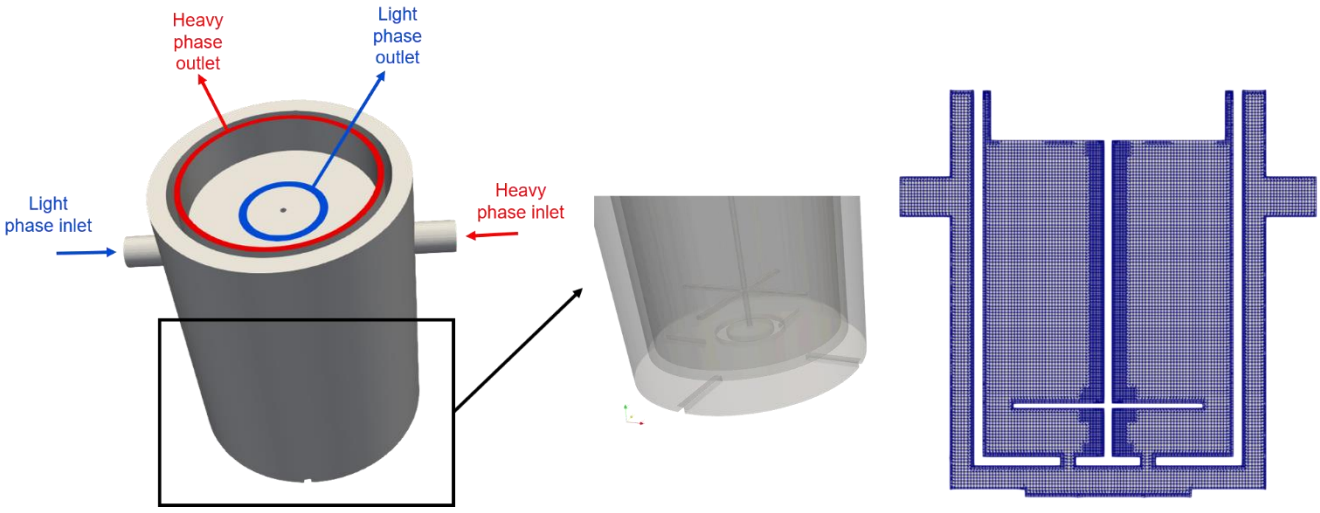

Figure 12. Computational domain for the ACC simulation.

Table 1. Physical properties of the two phases.

	Density (kg/m^3)	Dynamic viscosity (Pa s)
TBP/dodecane	806	1.894e-3
Nitric acid	1110	1.129e-3
Surface tension (N/m)	0.00983	

A tributyl phosphate(TBP)/dodecane mixture at 30/70 wt% and nitric acid (HNO_3) are assumed to represent the light organic phase and the heavy aqueous phase, respectively. The physical properties of the two phases are reported in Table 1. The aqueous over organic volumetric flow rate ratio is equal to 2:1. The rotating speed of

This project has received funding from the EURATOM research and training programme 2014-2018 under grant agreement No 730227

the rotor is equal to 3600 RPM. The Moving Reference Frame (MRF) approach is used to account for the rotation in the numerical simulation.

Both TBP/dodecane and nitric acid are considered to be turbulent, and a wall-modelled LES approach with the a dynamic Smagorinsky [41] closure for the subgrid-scale stresses is used for both phases. The diameter of the TBP/dodecane phase is evaluated using the OPOSPM population balance. After an initial transient of 3.5 seconds, the flow in the system was observed to have reached a statistically-steady state. After the initial transient, flow statistics have been collected for 4 seconds, leading to a total 7.5 seconds of simulated flow time.

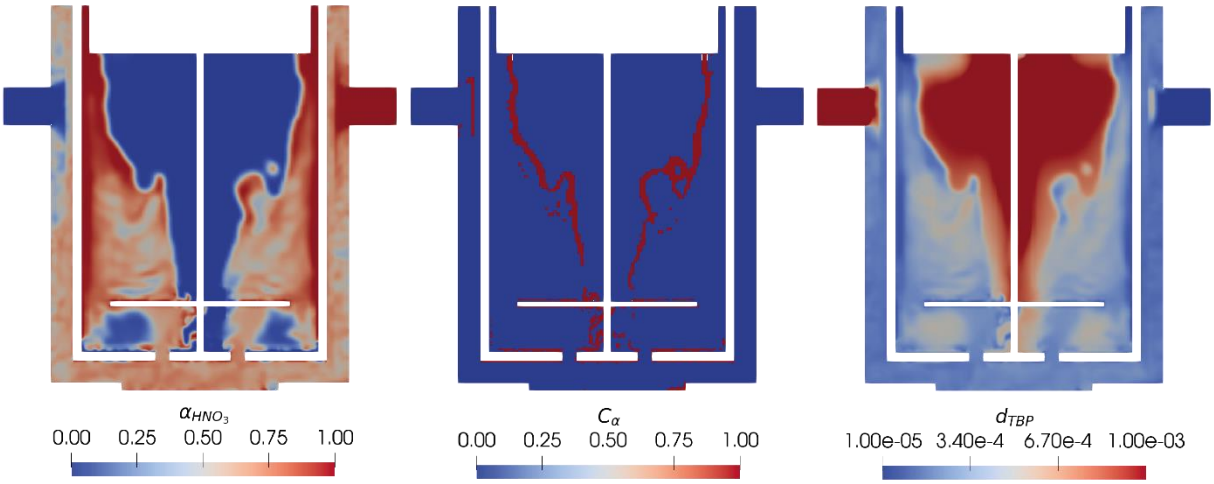

Figure 13. Instantaneous contours of HNO3 volume fraction, C_α switch and diameter of the dispersed phase on the ACC mid-plane.

The instantaneous contours of the heavy phase volume fraction, C_α switch and light phase diameter on the ACC vertical mid-plane are shown in Figure 13. The instantaneous HNO_3 contours within the annulus show that any information on the interface morphology is lost, and this is due to the fact that the model is working in small/dispersed-interface mode in that region. This is confirmed by the C_α contour plots, which shows that the switch is set to zero almost everywhere within the annulus. Moving within the rotor, it can be seen that due to coalescence of the organic phase and the consequent increase in d_{TBP}, the C_α switch tends to assume a unity value at the interface between the two phases; this is particularly evident in the upper part of the rotor, where the typical cone-shaped interface typical of ACCs [4] can be observed and complete phase separation is achieved. The activation of the C_α switch within the rotor allows for the model to work in large-interface mode; this results in a direct resolution of the interface morphology, as it can be inferred by the sharp interface shown in the α_{HNO_3} contour plots in the upper part of rotor. With respect to the organic phase diameter, it should be pointed out that the contours shown in Figure 13 report the diameter obtained from the OPOSPM population balance; even if this diameter is defined everywhere in the domain, it is only representative of the interfacial scales in the regions where C_α is equal to zero. In the large-interface cells, the interfacial morphology is directly resolved and therefore the interfacial scales should be evaluated directly from the volume fraction field. In these cells Equation (14) is no longer valid, and the interfacial area density is given by

$$a_i = |\nabla \alpha| \tag{15}$$

Figure 14 shows the time-averaged contours of the HNO_3 volume fraction and of the TBP/dodecane phase diameter. From the time-averaged heavy phase volume fraction contours, it is observed that a fine dispersion is established within the annulus, as confirmed by the time-averaged diameter contours; within the rotor, due to coalescence and separation, a cone-shaped interface is observed, with a well-defined dispersion band located

This project has received funding from the EURATOM research and training programme 2014-2018 under grant agreement No 730227

between the heavy phase and the light phase outlets, and a complete disengagement of the two phases at the top of the rotor.

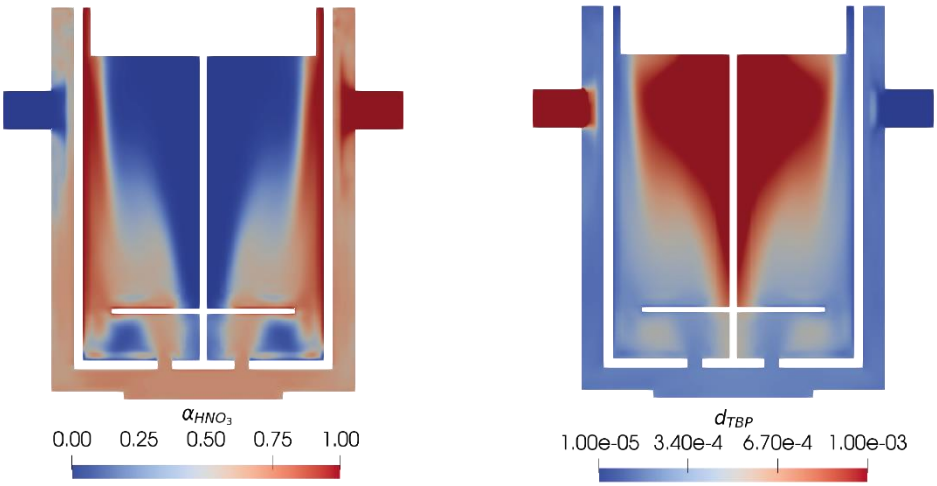

Figure 14. Time-averaged contours of HNO3 volume fraction and C_α switch on the ACC mid-plane.

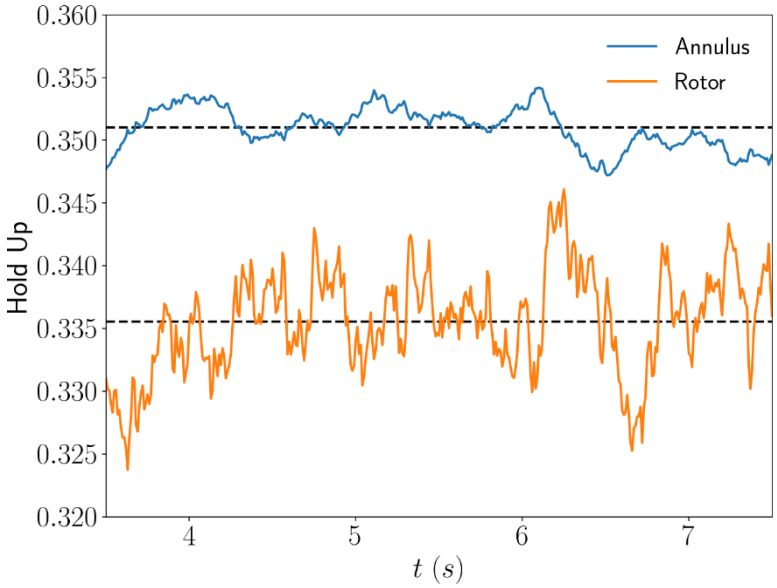

Figure 15. Transient evolution of the organic phase hold-up in the annulus and in the rotor.

The evolution of the organic phase hold-up over time is shown in Figure 15. It can be observed that the hold-up has reached a statistically steady-state in both the annulus and the rotor during the sampling time spanning from t=3.5 to t=7.5 seconds. The time-averaged hold-up values are equal to 0.351 and 0.336 in the annulus and in the rotor, respectively, thus the hold-up the annulus is higher by 4.3% with respect to the value observed within the rotor.

Figure 16 shows the evolution of the (spatially) average organic phase diameter within the annulus over time. It can be observed that also this quantity shows a statistically steady-state behaviour over the sampling time. The time-averaged diameter value in the annulus is equal to 0.165 mm. For comparison, the mean diameter evaluated with the correlation proposed by [42] is 0.243 mm. The correlation is given as

This project has received funding from the EURATOM research and training programme 2014-2018 under grant agreement No 730227

$$\frac{d}{g} = 150(We)^{-0.65}(Re)^{-0.2}\left(\frac{\mu_d}{\mu_c}\right)^{0.5}\left(\frac{g}{D_i}\right)^{0.5} \quad (16)$$

where We and Re are the droplet Weber and Reynolds number, respectively, D_i is the inner diameter of the annulus and g is the annulus gap.

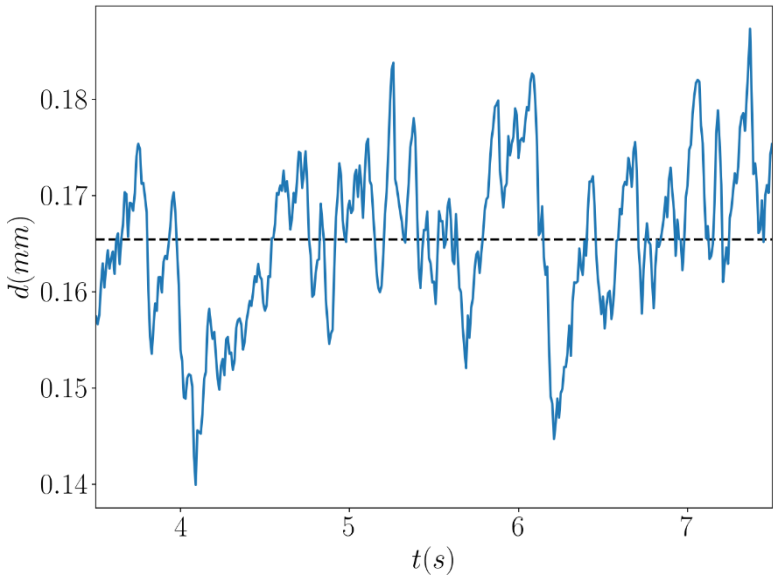

Figure 16. Transient evolution of the average organic phase diameter in the annulus.

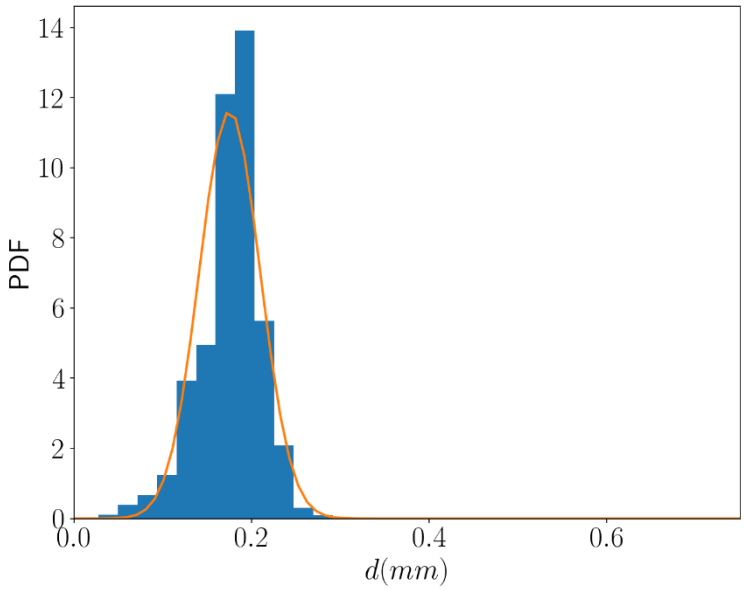

Figure 17. Instantaneous droplet size distribution within the annulus at $t = 7.5\ s$.

The instantaneous organic phase droplet size distribution within the annulus at $t = 7.5\ s$ is shown in Figure 17. The spatially-averaged instantaneous diameter is equal to 0.175 mm at the considered time. The diameter PDF shape is in qualitative good agreement with the size distributions that have been observed experimentally in ACCs [29] [39], which confirmed the ability of the GEMMA approach coupled with OPOSPM to provide a reliable prediction of the expected droplet size distribution observed in the mixing section of ACCs.

This project has received funding from the EURATOM research and training programme 2014-2018 under grant agreement No 730227

CONCLUSIONS

The flow observed in intensified liquid-liquid extraction devices such as Annular Centrifugal Contactors is very complex and not fully understood. Computational Fluid Dynamics can be a valuable tool to gain useful insights on the hydrodynamic behaviour of these devices. However, the multiscale nature of the multiphase flows observed in Annular Centrifugal Contactors rules out the use of standard “off-the-shelf” multiphase models, that usually assume either small interfacial scales (in the case if dispersed flows) or large interfacial scales (in the case of segregated flows) with respect to the local spatial resolution of the numerical grid.

Consequently, the University of Leeds has developed and assessed a novel GEneralized Multifluid Modelling Approach (GEMMA) which aims to overcome the limitations of the standard approaches in the simulation of multiscale flows such as those observed in Annular Centrifugal Contactors. The proposed approach uses a binary function to switch between large-interface and small-interface mode locally. The switch status also controls relevant terms in the governing equations such as the surface tension force and the blending between interfacial transfer models suitable for small/dispersed and large/segregated interfaces. The switch logic is based on the evaluation of the local resolution of the interfacial scales.

Preliminarily, the proposed modelling approach has been assessed in different test cases and demonstrated to have an accuracy comparable to standard interface-resolving approaches such as VoF in typical large/segregated-interface flow cases; the ability of the approach to deal with multiscale flows and switch between large-interface and small-interface mode locally has been demonstrated in a prototypical multiscale flow.

Successively, the GEMMA approach has been used to simulate the flow in the mixing region of a centrifugal contactor at different rotating speeds. It has been demonstrated that the proposed approach is capable of reproducing the main hydrodynamic features observed in such flows. Further, it has been shown that the GEMMA approach coupled with a reduced population balance provides a good estimation of the dispersed phase droplet size measured experimentally.

Finally, the operation of a lab-scale Annular Centrifugal Contactor has been simulated. It has been observed that the proposed modelling approach can seamlessly switch between a small-interface formulation in the annulus and a large-interface formulation within the rotor. This allows for an accurate prediction of the droplet size distribution in the mixing region; at the same time, a reliable prediction of the interface morphology, and thus of the dispersion band, can be attained within the rotor.

Overall, it has been demonstrated that the GEMMA approach represents a pragmatic tool for the evaluation of the complex hydrodynamic features of the multiscale flow observed in Annular Centrifugal Contactors. Future work will include further assessment of the model against experimental observations and the implementation and validation of mass transfer prediction capabilities within the modelling approach.

BIBLIOGRAPHY

[1] B. Hanson, “Process engineering and design for spent nuclear fuel reprocessing and recycling plants,” in *Reprocessing and Recycling of Spent Nuclear Fuel*, R. Taylor, Ed., Oxford, Woodhead Publishing, 2015, pp.

This project has received funding from the EURATOM research and training programme 2014-2018 under grant agreement No 730227

125-151.

[2] E. Müller, R. Berger, E. Blass, D. Sluyts and A. Pfennig, "Liquid–Liquid Extraction," in *Ullmann's Encyclopedia of Industrial Chemistry*, vol. 21, 2008, pp. 249-307.

[3] R. A. Leonard, "Design Principles and Applications of Centrifugal Contactors for Solvent Extraction," in *Ion Exchange and Solvent Extraction*, B. Moyer, Ed., Boca Raton, CRC Press, 2010, pp. 564-613.

[4] S. Vedantam and J. B. Joshi, "Annular Centrifugal Contactors — A Review," *Chemical Engineering Research and Design,* vol. 84, pp. 522-542, 2006.

[5] S. Vedantam, K. E. Wardle, T. V. Tamhane, V. V. Ranade and J. B. Joshi, "CFD Simulation of Annular Centrifugal Extractors," *International Journal of Chemical Engineering,* vol. 2012, 2012.

[6] H. Marschall, "Towards the numerical simulation of multi-scale two-phase flows," 2011.

[7] A. Prosperetti and G. Tryggvason, Computational Methods for Multiphase Flow, Cambridge: Cambridge University Press, 2007.

[8] M. Sussman and E. G. Puckett, "A Coupled Level Set and Volume-of-Fluid Method for Computing 3D and Axisymmetric Incompressible Two-Phase Flows," *Journal of Computational Physics,* vol. 162, pp. 301-337, 2000.

[9] C. W. Hirt and B. D. Nichols, "Volume of fluid VOF method for the dynamics of free boundaries," *Journal of Computational Physics,* vol. 39, pp. 201-225, 1981.

[10] D. W. Theobald, B. Hanson, M. Fairweather and P. J. Heggs, "Implications of hydrodynamics on the design of pulsed sieve-plate extraction columns: A one-fluid multiphase CFD model using the volume of fluid method," *Chemical Engineering Science,* vol. 221, p. 115640, 2020.

[11] K. E. Wardle, "Open-Source CFD Simulations of Liquid–Liquid Flow in the Annular Centrifugal Contactor," *Separation Science and Technology,* vol. 46, pp. 2409-2417, 2011.

[12] G. Cerne, S. Petelin and I. Tiselj, "Coupling of the Interface Tracking and the Two-Fluid Models for the Simulation of Incompressible Two-Phase Flow," *Journal of Computational Physics,* vol. 171, pp. 776-804, 2001.

[13] K. E. Wardle and H. G. Weller, "Hybrid Multiphase CFD Solver for Coupled Dispersed/Segregated Flows in Liquid-Liquid Extraction," *International Journal of Chemical Engineering,* vol. 2013, pp. 1-13, 2013.

This project has received funding from the EURATOM research and training programme 2014-2018 under grant agreement No 730227

[14] A. De Santis, M. Colombo, B. C. Hanson and M. Fairweather, "A generalized multiphase modelling approach for multiscale flows," *Journal of Computational Physics,* 2020.

[15] H. G. Weller, G. Tabor, H. Jasak and C. Fureby, "A tensorial approach to computational continuum mechanics using object-oriented techniques," *Computers in Physics,* vol. 12, pp. 620-631, 1998.

[16] The OpenFOAM Foundation, "OpenFOAM - User Guide," 2019.

[17] E. Krepper, D. Lucas, T. Frank, H.-M. Prasser and P. J. Zwart, "The inhomogeneous MUSIG model for the simulation of polydispersed flows," *Nuclear Engineering and Design,* vol. 238, p. 1690–1702, 2008.

[18] L. Schiller and A. Naumann, "A drag coefficient correlation," *Zeitschrift des Vereins Deutscher Ingenieure,* vol. 77, pp. 318-320, 1935.

[19] E. Berberovic, N. P. van Hinsberg, S. Jakirlic, I. V. Roisman and C. Tropea, "Drop impact onto a liquid layer of finite thickness: Dynamics of the cavity evolution," *Physical Review E,* vol. 79, p. 036306, 2009.

[20] J. U. Brackbill, D. B. Kothe and C. Zemach, "A continuum method for modeling surface tension," *Journal of computational physics,* vol. 100, p. 335–354, 1992.

[21] J. A. Heyns and O. F. Oxtoby, "Modelling surface tension dominated multiphase flows using the VOF approach," in *6th European Conference on Computational Fluid Dynamics*, 2014.

[22] O. Ubbink, "Numerical prediction of two fluid systems with sharp interfaces," 1997.

[23] L. Štrubelj, I. Tiselj and B. Mavko, "Simulations of free surface flows with implementation of surface tension and interface sharpening in the two-fluid model," *International Journal of Heat and Fluid Flow,* vol. 30, p. 741–750, 2009.

[24] J. Anez, F. Demoulin, N. Hecht and J. Reveillon, "A general purpose LES model for atomization," in *European Conference Liquid Atomization & Spray Systems*, 2016.

[25] C. Drumm, M. Attarakih, M. W. Hlawitschka and H.-J. Bart, "One-Group Reduced Population Balance Model for CFD Simulation of a Pilot-Plant Extraction Column," *Industrial and Engineering Chemistry Research,* vol. 49, p. 3442–3451, 2010.

[26] M. M. Attarakih, C. Drumm and H. Bart, "Solution of the population balance equation using the sectional quadrature method of moments (SQMOM)," *Chemical Engineering Science,* vol. 64, pp. 742-752, 2009.

This project has received funding from the EURATOM research and training programme 2014-2018 under grant agreement No 730227

[27] C. Martinez-Bazan, J. L. Montanes and J. C. Lasheras, "On the breakup of an air bubble injected into a fully developed turbulent flow," *Journal of Fluid Mechanics,* vol. 401, p. 157–182, 1999.

[28] M. J. Prince and H. W. Blanch, "Bubble coalescence and break-up in air-sparged bubble columns," *AIChE Journal,* vol. 36, pp. 1485-1499, 1990.

[29] K. E. Wardle, "Hybrid multiphase CFD simulation for liquid-liquid interfacial area prediction in annular centrifugal contactors," in *Proceeding of the Global 2013*, Salt Lake City, Usa, 2013.

[30] A. Mathur, D. Dovizio, E. M. A. Frederix and E. M. J. Komen, "A Hybrid Dispersed-Large Interface Solver for multi-scale two-phase flow modelling," *Nuclear Engineering and Design,* vol. 344, p. 69–82, 2019.

[31] S. Hänsch, D. Lucas, T. Höhne and E. Krepper, "Application of a new concept for multi-scale interfacial structures to the dam-break case with an obstacle," *Nuclear Engineering and Design,* vol. 279, pp. 171-181, 2014.

[32] C. H. Yu, H. L. Wen, Z. H. Gu and R. D. An, "Numerical simulation of dam-break flow impacting a stationary obstacle by a CLSVOF/IB method," *Communications in Nonlinear Science and Numerical Simulation,* vol. 79, p. 104934, 2019.

[33] S. Koshizuka, H. Tamako and Y. Oka, "A particle method for incompressible viscousflow with fluid fragmentation," *International Journal of Computational Fluid Dynamics,* vol. 4, pp. 29-46, 1995.

[34] Y. Zhu, H. N. Oguz and A. Prosperetti, "On the mechanism of air entrainment by liquid jets at a free surface," *Journal of Fluid Mechanics,* vol. 404, p. 151–177, 2000.

[35] S. Hänsch, D. Lucas, E. Krepper and T. Höhne, "A multi-field two-fluid concept for transitions between different scales of interfacial structures," *International Journal of Multiphase Flow,* vol. 47, p. 171–182, 2012.

[36] O. Y. Shonibare and K. E. Wardle, "Numerical Investigation of Vertical Plunging Jet Using a Hybrid Multifluid–VOF Multiphase CFD Solver," *International Journal of Chemical Engineering,* vol. 2015, pp. 1-14, 2015.

[37] X. L. Qu, L. Khezzar, D. Danciu, M. Labois and D. Lakehal, "Characterization of plunging liquid jets: A combined experimental and numerical investigation," *International Journal of Multiphase Flow,* vol. 37, pp. 722-731, 2011.

[38] J. Smagorinsky, "General Circulation Experiments With the Primitive Equations," *Monthly Weather Review,*

vol. 91, p. 99–164, 1963.

[39] N. B. Wyatt, T. J. O'Hern and B. Shelden, “Drop-size distributions and spatial distributions in an annular centrifugal contactor,” *AIChE Journal,* vol. 59, pp. 2219-2226, 2013.

[40] B. E. Launder and D. B. Spalding, “The numerical computation of turbulent flows,” *Computer Methods in Applied Mechanics and Engineering,* vol. 3, pp. 269-289, 1974.

[41] A. Verma and K. Mahesh, “A Lagrangian subgrid-scale model with dynamic estimation of Lagrangian time scale for large eddy simulation of complex flows,” *Physics of Fluids,* vol. 24, p. 085101, 2012.

[42] P. A. Haas, “Turbulent dispersion of aqueous drops in organic liquids,” *AIChE Journal,* vol. 33, pp. 987-995, 1987.

This project has received funding from the EURATOM research and training programme 2014-2018 under grant agreement No 730227